Sensors and Materials, Vol. 29, No. 8 (2017) 1109–1122
MYU Tokyo

S & M 1404

Study of Space Charge Dynamics in Oil and Pressboard Composite System under Different Polarity Reversal Voltages

Miao Hao,* George Chen, Xin Chen,[1] Chong Zhang,[1]
Wenpeng Li,[1] Haitian Wang,[1] Mingyu Zhou,[1] and Xianzhang Lei[1]

University of Southampton, University Road, Southampton, SO17 2GR, United Kingdom
[1]Global Energy Interconnection Research Institute, Beijing, 102200, China

(Received June 27, 2016; accepted March 22, 2017)

Keywords: polarity reversal, oil-pressboard, aging, space charge, PEA, HVDC, dilectrics, electric field distortion, interface

The impacts caused by the polarity reversal of the applied voltage on space charge dynamics and electric field enhancement across an oil gap have been studied in an oil gap and single-layer pressboard composite insulation system. The experimental results validate that the electric field enhancement across the oil gap immediately after the application of the reversed electric field is directly dependent on the number of residual charges within the insulation system at the moment of the application of the reversed stress. Therefore, the electric field enhancement in the system is strongly dependent on the magnitude of the applied electric field, the duration of polarity reversal and the degradation of the mineral oil. An estimation of the enhanced electric field immediately after polarity reversal based on the charge decay characteristics has been proposed and successfully applied to calculate the electric field enhancement in an aged oil sample under 20 kV/mm, which cannot be accurately measured due to the very fast space charge dynamics in the aged oil under a strongly enhanced electric field.

1. Introduction

Polarity reversal operation, which allows the control of the direction of power flow, is one of the most important functions of the high-voltage direct current (HVDC) transmission for the development of a global power network and power trade. From the viewpoint of dielectric properties, polarity reversal stress is a critical condition that challenges the reliability of the insulation system in various types of HVDC equipment, such as converter transformers and cables.[(1)] In recent years, many studies have demonstrated that the accumulated charges can rapidly enhance the electric field after polarity reversal in the polymeric materials used for HVDC cables.[(2–4)] On the other hand, the dielectric properties of oil/paper and oil-paper composite systems, which are widely used in converter transformers, can be significantly influenced by space charge characteristics.[(5–11)] The accumulation of space charge at the interfaces and in the bulk solid parts of an oil-paper composite insulation system can greatly enhance the electric field distributed in the central region of the paper. Similarly to polymeric materials, researchers also found that the accumulated homocharges in a single layer of impregnated paper/pressboard with oil can lead to electric field enhancement in the surface region after polarity reversal.[(12–15)] However, in a real converter transformer, the insulation system is much more complex, i.e., thick pressboards

*Corresponding author: e-mail: m.hao@soton.ac.uk
http://dx.doi.org/10.18494/SAM.2017.1422

ISSN 0914-4935 © MYU K.K.

are immersed in a large quantity of insulating oil. Under such complex conditions, space charge characteristics under polarity reversal stress are still poorly understood and difficult to estimate.

In the present study, the pulsed electroacoustic (PEA) technique has been used to investigate space charge dynamics in an oil-impregnated pressboard with a thickness of 1 mm combined with a 0.5-mm-thick oil film under different polarity reversal stresses at room temperature. A method for estimating the space charge distribution, based on space charge characteristics, is proposed and validated.

2. Polarity Reversal Process

Based on the understanding of space charge build-up and decay characteristics in oil-pressboard composite systems, the whole polarity reversal operation can be divided into three stages, as shown in Fig. 1. The different origins of the charges are shown in Fig. 1(b) to clearly demonstrate the complex dynamics of the space charge during the whole polarity reversal process. However, different types of charge within a similar region, such as electrodes, will recombine with each other, and only net charges can be measured by the PEA system.

Stage 1: When an external HVDC electric field ($+U$) is applied, space charges will be injected and accumulated in the oil-pressboard insulation system. The space charge characteristics are the same as the charge behavior under a constant HVDC stress, as illustrated in a previous paper.[6] Homocharges are injected from the electrodes and then accumulate at the oil/pressboard interface and the bulk of the pressboard. The amount of accumulated charges is strongly dependent on the magnitude and duration of the electric field application and the ageing status of the dielectrics.

Stage 2: In this stage, a short period is used for polarity reversal. IEC-61378-2 only requires that the whole polarity reversal process should be completed within 2 min.[16] The power industry usually turns off the applied voltage first, and then turns on the voltage with the opposite polarity after 2 min. In this study, for simplisity, the external voltage is directly removed during this stage. Therefore, this stage can be simply regarded as a charge decay process during this short period of time.

Stage 3: In this stage, the HVDC voltage with the opposite polarity ($-U$) is applied. The residual charges in the insulation bulk act as heterocharges under the $-U$ voltage and enhance the electric field in the vicinity of the two electrodes. With further application of the $-U$ voltage, the enhanced electric field near the electrodes could lead to a stronger charge injection to neutralize these heterocharges and reach a new balance of space charge dynamics.

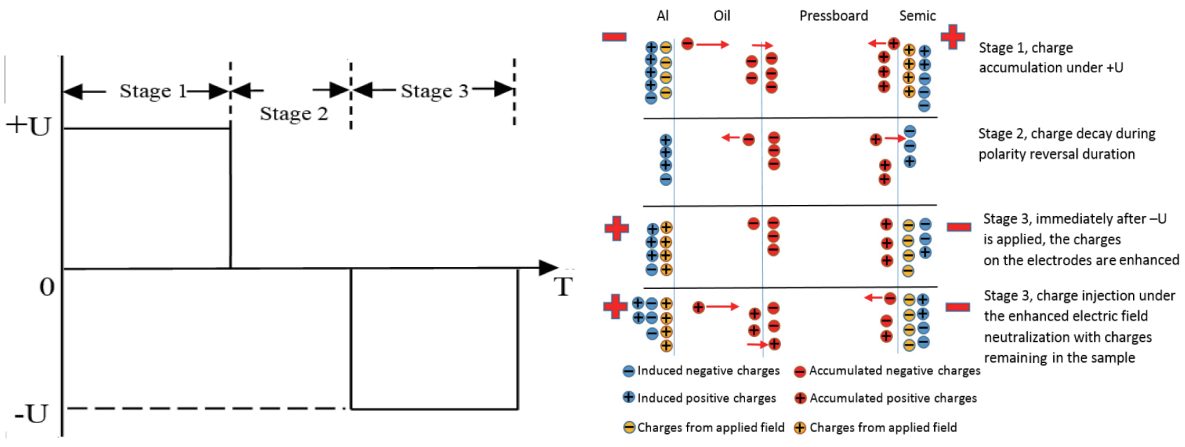

(a) (b)

Fig. 1. (Color online) Three stages of polarity reversal voltage (a) and charge dynamics (b).

With this polarity reversal operation, the electric field will be significantly enhanced immediately after the polarity reversal, i.e., the start of stage 3. The magnitude of the enhanced electric field strongly depends on the amount of residual charges after stage 2, which is further related to the space charge characteristics of the dielectrics. Therefore, we will experimentally validate the charge behavior in the proposed three-stage polarity reversal process. Then, some important factors related to the space charge behavior are investigated regarding the electric field enhancement after polarity reversal, such as the magnitude of the external voltage, the duration of stage 2 and the ageing status of the insulating oil.

3. Experimental Setup

3.1 Sample preparation

To investigate the impacts of the ageing status of the mineral oil on the electric field enhancement after polarity reversal, both fresh oil and aged oil were used for comparison. The characteristics of the two types of oil are shown in Table 1. The pressboards used in this study were the generally available transformer pressboards with a thickness of 1 mm and a pressed pattern surface. The pressboards were cut into circular shapes with a diameter of 9 cm, and then dried at 80 ℃ for 3 d in a vacuum oven. After that, the dried pressboards were separately impregnated in the two types of oil under 10 Pa/60 ℃ for 3 d, after which, the pressboards were fully impregnated with oil. The unused impregnated pressboards were kept in a sealed container under vacuum condition to prevent them from absorbing moisture and impurities. The dielectric properties of the impregnated pressboards are shown in Table 2. The details of the sample preparation and characterization can be found in Ref. 6.

3.2 Experimental method

The setup of the PEA measurement is shown in Fig. 2(a). A 0.5-mm-thick PTFE ring was placed at the bottom of the container to create an oil gap. The pressboard was firmly pressed by the top electrode with a controlled and repeatable pressure above the oil gap, in order to achieve a good contact between the electrode and different layers of dielectrics. This is essential for acoustic signal transmission and ensures a good repeatability of the measurements. The high-voltage pulse signal used in this work has a voltage of 1 kV and a pulse width of 5 ns with a repetition rate of 1 kHz. The space charge caused by the pulse stress can be ignored and no obvious acoustic reflection can be observed in the original signal under only pulse stress. Note that the results in this work were recovered from the displacement field distribution within the two different dielectric materials, and the impacts of the different speeds of sound in the two materials were considered, based on the method introduced in Refs. 12 and 16. However, the influences of the acoustic attenuation and dispersion were not recovered, leading to an inaccurate space charge density, near the top electrode, but the trend of the charge dynamics remains the same.

Table 1
Status of the oil properties.

	Fresh oil	Aged oil
Moisture (ppm)	10	25
Resistivity (TΩm)	7	0.1
Relative permittivity	2.2	2.6
Description	Transparent	Dark brown with sludge

Table 2
Dielectric properties of the impregnated pressboards.

	Fresh oil-PB	Aged oil-PB
Resistivity (TΩm)	140	0.3
Relative permittivity	3.2	4.2

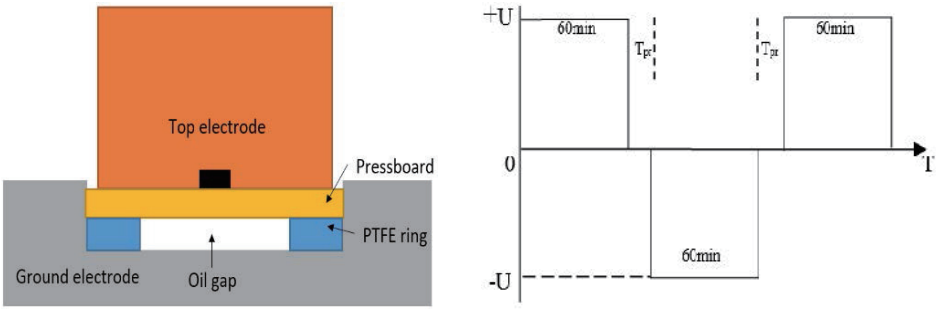

(a) (b)

Fig. 2. (Color online) Measurement setup (a) and procedures of voltage polarity reversal (b).

The applied voltage profile is shown in Fig. 2(b). First, $+U$ was applied for 60 min, and then, the voltage was turned off and waited for the time T_{pr} to allow charge decay. After that, the voltage $-U$ was turned on for another 60 min, then the processes were repeated with the voltage to $+U$ again. The effects of the following parameters on the charge dynamics were investigated: (i) the magnitude of the applied voltage, U, was set to 18 kV (12 kV/mm) or 30 kV (20 kV/mm) and (ii) the duration of polarity reversal, T_{pr}, was 0.5, 2, or 5 min in this work. Two reversals are required in IEC-61378-2 to test an unsymmetrical insulation structure and other impacts caused by polarity-dependent phenomena.[17]

4. Results and Discussion

4.1 Space charge dynamics under polarity reversal voltage

In this section, the proposed space charge dynamics during the polarity reversal operation is verified by PEA measurements in a fresh oil sample. The applied electric field is 20 kV/mm, and the duration of polarity reversal is 2 min.

The charge dynamics in the fresh oil sample observed before and after the first polarity reversal ($+U$ to $-U$) are shown in Fig. 3(a), while those observed before and after the second polarity reversal ($-U$ to $+U$) are shown in Fig. 3(b). The black arrows indicate the trend before polarity reversal, while the red arrows show the trend after polarity reversal.

According to Fig. 3(a), negative charges are injected from the ground (Al) electrode and accumulate at the oil and pressboard interface. However, the amount of interfacial charges is small due to the short duration of DC voltage application and good dielectric properties. Thus, after polarity reversal, the charge density at the Al electrode is enhanced to about 10 C/m^3 as the accumulated charges remain in the insulation bulk, especially in the vicinity of the interface. Immediately after the application of the reversed voltage, the interfacial peak is divided into two parts. The first part seems to be located in the oil gap, which can be quickly reversed to the same polarity as the applied voltage. The other part originates from the charges accumulating within the pressboard bulk, which cannot quickly dissipate but enhance the electric field across the oil gap. The electric field across the oil gap is positively proportional to the magnitude of the ground electrode peak, which is shown in Ref. 6. The enhanced electric field also results in more positive charges accumulating at the interface after the first polarity reversal. In the vicinity of the top (semiconducting polymer) electrode, the amount of accumulated negative charges under the negative voltage is also higher than that under the positive voltage, although the signal is severely

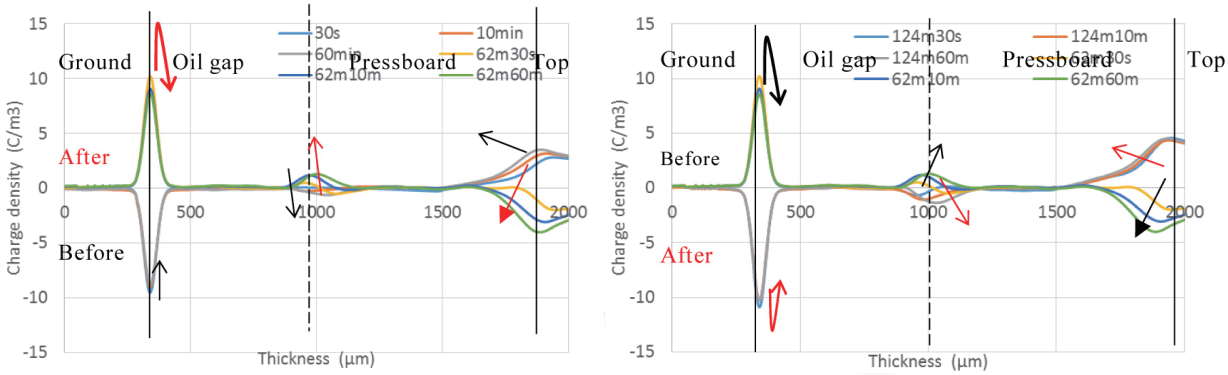

Fig. 3. (Color online) Space charge dynamics observed before and after the first (a) and second (b) polarity reversal processes.

attenuated. This could also result from the enhanced electric field at the interface between the pressboard and the top electrode. Moreover, the different characteristics for the positive and negative charges could be another possible reason. However, these differences are usually very small as mentioned in Ref. 5.

When the second polarity reversal operation is finished, the applied electric field reverses to +20 kV/mm again, as shown in Fig. 3(b). An almost symmetric space charge profile can be observed, similarly to that for the first polarity reversal, which is also known as the "mirror image effect".[4] Again, the interfacial charges in the oil gap can rapidly change to negative charges following the polarity of the ground electrode. The positive charges within the pressboard induce more negative charges at the ground electrode, leading to a slightly larger negative peak (about 1.1 C/m^3) than the peak after the first polarity reversal. The negative charges are then injected from the ground electrode. These injected negative charges gradually neutralize and replace the accumulated positive charges remaining in the pressboard bulk in the vicinity of the interface until the balance of the new charge dynamics is achieved.

Based on the results of the long-duration measurements in Ref. 6, the time for the dynamics balance of the space charges in the thick fresh oil sample is more than 24 h for an electric field of 12 kV/mm. However, only 1 h is applied in this work, resulting in the limited amount of space charges accumulating in the insulation bulk and the small field enhancement (which can be simply and approximately related to the amplitude of the peak at the ground electrode) after polarity reversal.

According to the three-stage process, on the other hand, the space charge profile immediately after polarity reversal can also be estimated based on the space charge profiles under 20 kV/mm DC stress in Ref. 6. The space charge distribution $\rho_{d(x)}$ after 2 min charge decay can be obtained from the previous charge decay result. The reversed voltage can be calculated from the reference data and voltage difference ratio.

The voltage difference ratio can be simply calculated as

$$R = \frac{U_{pr}}{U_{ref}}, \tag{1}$$

where U_{pr} is the polarity reversal voltage, which is −30 kV for the first polarity reversal, and U_{ref} is the reference voltage (+15 kV).

Therefore, the space charge profile after 2 min polarity reversal can be calculated as

$$\rho_{pr}(x) = \rho_d(x) + R \bullet \rho_{ref}(x), \tag{2}$$

where $\rho_{pr}(x)$ is the space charge profile after polarity reversal and $\rho_{ref}(x)$ is the space charge profile of the reference data.

Comparison of the estimated and experimental results is shown in Fig. 4. The estimated magnitude of the ground electrode is slightly higher than the experimental result. Moreover, only negative interfacial charges can be observed for the estimated result, while both positive and negative charges can be found in the vicinity of the interface. As explained previously, these positive interfacial charges are rapidly injected from the ground electrode due to the enhanced electric field across the oil gap during the first 30 s (including the time to collect the experimental data) immediately after the application of the polarity reversal voltage. These rapidly injected positive charges neutralize some of the accumulated negative charges and also slightly reduce the magnitude of the peak of the ground electrode. This indicates that the measurement results cannot accurately show the space charge distribution and the maximum electric field of the first moment after polarity reversal, due to the delay of the data acquisition duration. Therefore, the estimated result may be close to the real conditions when the reversed voltage is immediately applied. Also note that the estimated data was calculated from the results of 3 h voltage application, which obviously leads to more accumulated charges within the insulation system, inducing more positive charges on the ground electrode. However, considering that the total amount of charges in the fresh oil sample is very small and the charge movement in the fresh oil sample is generally slow, this difference is also very small. In contrast, the estimated and measurement results are very different when the charge movement is very quick, for example, in the aged oil samples (shown in the following sections).

4.2 Impacts of the magnitude of the applied electric field

It is generally believed that a high electric field can increase the amount of space charges within a dielectric material by both increasing the charge injection based on Schottky injection and enhancing the charge mobility, which also leads to a higher conductivity. This suggests that more heterocharges accumulate in the insulation system, which can potentially increase the electric field distortion after polarity reversal.

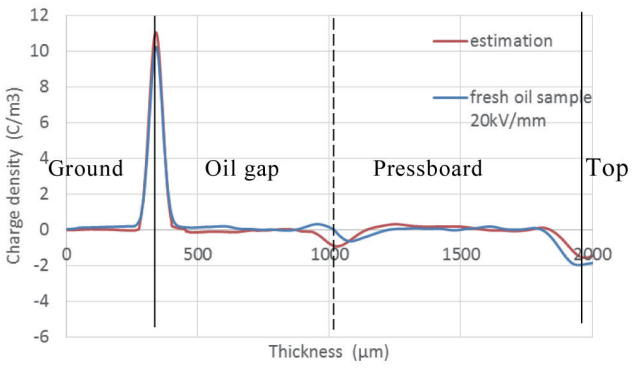

Fig. 4. (Color online) Comparison between the measurement and estimated space charge distributions immediately after the first polarity reversal in the fresh oil sample under 20 kV/mm with T_{pr} = 2 min.

In this section, the impacts caused by the electric fields of 12 and 20 kV/mm in the fresh and aged oil samples are investigated separately. The duration of polarity reversal is fixed to 30 s.

Figure 5(a) shows space charge distributions in the fresh oil sample under different electric fields immediately after the first polarity reversal (from $+U$ to $-U$). It can be clearly observed that more heterocharges (negative charges) remain in the vicinity of the oil/pressboard interface, which can induce more positive charges at the ground electrode. More positive charges can also be found at the interface on the oil side. As explained previously, these positive charges are injected from the ground electrode during the short period (30 s) for the data acquisition process of the oscilloscope after the application of the reversed voltage (the ground electrode now is the anode). Therefore, a large number of positive charges can directly indicate the enhancement of charge injection and mobility caused by a high electric field, compared with the result obtained under a low electric field.

The electric field distributions under 12 and 20 kV/mm are calculated from the space charge profiles, as shown in Fig. 5(b). Immediately after polarity reversal, the electric field within the oil gap is generally higher than that in the pressboard. The maximum electric field is located at the oil and pressboard interface as the positive charges are injected and accumulated at the interface, which is close to the residual negative charges in the pressboard.

Table 3 shows the electric field enhancement in the oil gap under different applied electric field magnitude. The electric field enhancement under a high electric field is slightly larger than that under a low electric field. The reader should be aware that the electric field enhancement calculations are based on the space charge distributions in Fig. 5(a), which can be affected by those positive charges injected within 30 s. These charges can reduce the electric field across the oil gap, especially under a high electric field. Therefore, the 'real' difference in electric field enhancement caused by the different applied electric field magnitudes may be larger.

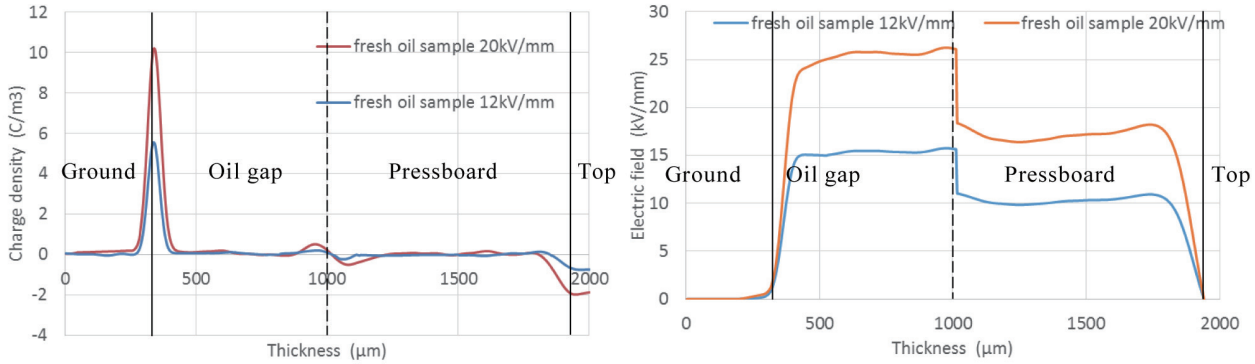

(a) (b)

Fig. 5. (Color online) Space charge (a) and electric field (b) distributions immediately after the first polarity reversal in the fresh oil sample under 12 and 20 kV/mm with T_{pr} = 30 s.

Table 3
Impacts of the magnitude of applied electric field in the fresh oil sample.

Applied electric field (kV/mm)	Peak value of ground electrode (C/m^3)	Maximum electric field (kV/mm)	Field enhancement in oil gap (%)
12	5.1	15.7	30.8
20	10.2	26.3	31.5

On the other hand, in the aged oil sample, the space charge distributions under different applied electric fields are shown in Fig. 6(a). Under 12 kV/mm, a considerable amount of heterocharges can be observed in the vicinity of the oil/pressboard and pressboard/top electrode interfaces, which greatly increases the magnitude of both peaks on the electrodes. However, no heterocharges can be observed in the insulation system, resulting in a limited increase in the magnitude of the ground electrode peak. Similarly to the fresh oil sample under a high electric field, the positive charge injection during the 30 s period for data acquisition is significantly enhanced by both the high reverse electric field and the aged oil. A significant drop of the peak on the ground electrode was observed during data acquisition in the experiments. Therefore, a more accurate way to describe the impact caused by the high electric field in the aged oil is to use the estimation method based on the DC space charge characteristics. This estimation method was introduced in the previous section, and the result is also shown in Fig. 6(a). It can be observed that a significant number of heterocharges exist in the insulation system, resulting in an enhanced peak value on the ground electrode (about 15 C/m^3). This result confirms the significant impact caused by the high electric field in the aged oil sample, and also shows the superiority of the estimation method over the measurement when the space charge dynamics are very fast, particularly in the aged oil sample under a high electric field.

The electric field distributions in the aged sample under different magnitudes of the applied electric field are shown in Fig. 6(b). Significant differences between the estimated and calculated electric field distributions based on the measured space charge profile under 20 kV/mm can be observed. The estimated electric field in the oil gap is around 40 kV/mm, and the maximum value is 42.1 kV/mm. However, the electric field calculated from the space charge distribution is around 20 kV/mm in the oil gap, and the maximum (25.2 kV/mm) occurs in the pressboard bulk, suggesting that a considerable number of homocharges were injected into the pressboard bulk. Under 12 kV/mm, the injection of the positive charges within 30 s may have also reduced the electric field in the oil gap. However, this reduction is not as significant as in the case of 20 kV/mm because the lower applied electric field can only be enhanced by a limited number of charges injected from that during the short period.

Table 4 shows the impacts caused by the different magnitudes of the applied electric field in the aged oil sample. The large difference in electric field enhancement between the lower electric field and the estimated result under the higher electric field indicates that the electric field impact was greater in the aged oil sample than in the fresh oil sample.

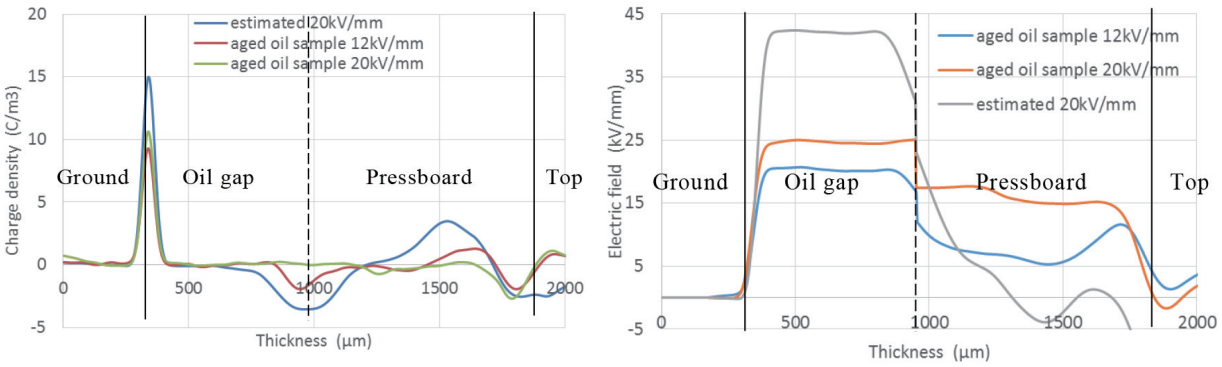

(a) (b)

Fig. 6. (Color online) Space charge (a) and electric field (b) distributions immediately after the first polarity reversal in the aged oil sample under 12 and 20 kV/mm with T_{pr} = 30 s.

Table 4
Impacts of the magnitude of the applied electric field in the aged oil sample.

Applied electric field (kV/mm)	Peak of ground electrode (C/m^3)	Maximum electric field (kV/mm)	Field enhancement in oil gap (%)
12	9.2	20.6	71.7
20	10.2	25.2	26
20 (estimated)	15.1	42.1	110.5

4.3 Impacts of the duration for polarityreversal

The accumulated charge dissipation can usually be described by an exponential function of the decay time.[5] However, the charge dissipation is also greatly dependent on the degradation of the mineral oil, i.e., the charges dissipate very slowly in the fresh oil sample, while they decay very rapidly in the aged oil sample.[6] Moreover, the oil and pressboard interface can potentially prevent charges from drifting away from the vicinity of the interface, acting as a barrier. However, this charge blocking effect is also greatly weakened in the aged oil sample. Therefore, the duration for charge dissipation may differently affect the space charge distribution in the fresh and aged oil samples. As a result, the electric field enhancement in the oil gap may be further influenced after polarity reversal.

In this section, the impact caused by the duration for polarity reversal is investigated and discussed from both experimental and estimated results in the fresh and aged oil samples.

4.3.1 Fresh oil sample under 20 kV/mm

Figure 7(a) shows space charge distributions in the fresh oil sample immediately after the application of the reversed electric field (from +20 to −20 kV/mm) with different polarity reversal durations, T_{pr}, i.e., 30 s, 2 min, and 5 min.

In general, the different polarity reversal durations have very little impacts on the charge dynamics in the fresh oil sample, because the charge dissipation is generally very slow in the fresh oil sample. A slight increase in negative peak at the ground electrode can be observed. This is caused by the larger amount of positive charges dissipated than negative charges within the same period, which is due to the fact that the positive charges can easily drift away from the electrode when they are in direct contact, while the accumulated negative charges in the vicinity of the oil and pressboard interface could be blocked (or deeply trapped). This phenomenon usually occurs in the first 30 min of charge dissipation in the fresh oil sample. This may result in an increase in electric field across the oil gap but a decrease in electric field in the vicinity of the interface between the pressboard and the top electrode, as shown in Fig. 7(b). However, the general impact is very limited since the amount of heterocharges in the fresh oil sample is very small. The impact of the duration of polarity reversal is summarized in Table 5. A limited impact (generally smaller than 40%) on the electric field enhancement in the oil gap can be found (the displacement field after polarity reversal dominates the field enhancement in the oil gap). It should also be noted that the impact of the polarity reversal duration is even smaller in the fresh oil sample under 12 kV/mm, in which the amount of heterocharges is much smaller.

4.3.2 Aged oil sample under 20 kV/mm

Under a high electric field, a large number of heterocharges exist in the insulation system, which can potentially greatly enhance the electric field across the oil gap. However, as explained

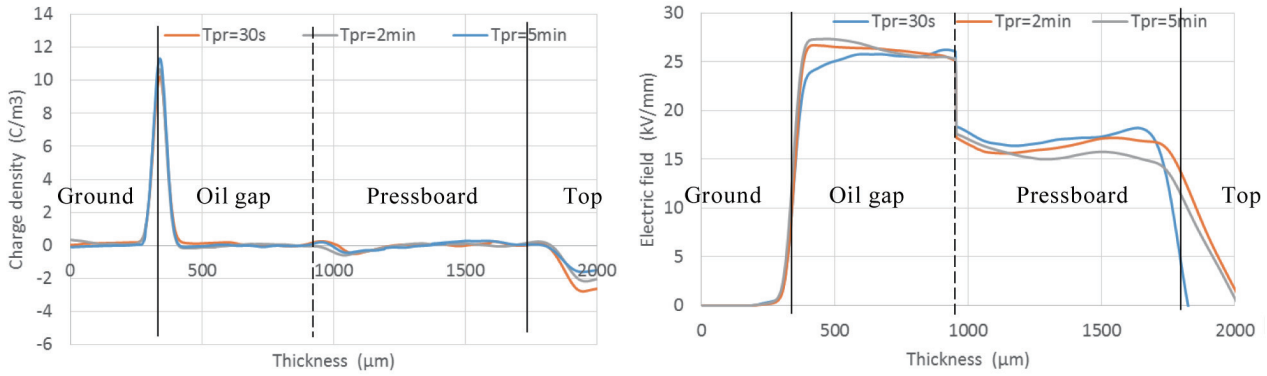

(a) (b)

Fig. 7. (Color online) Space charge (a) and electric field (b) distributions immediately after the first polarity reversal in the fresh oil sample under 20 kV/mm with T_{pr} = 30 s, 2 min, and 5 min.

Table 5
Impacts of the duration of polarity reversal in the fresh oil sample under 20 kV/mm.

Duration T_{pr} (min)	Peak of ground electrode (C/m^3)	Maximum electric field (kV/mm)	Field enhancement in oil gap (%)
0.5	10.2	26.3	31.5
2	10.7	27.1	35.5
5	11.3	27.4	37

previously, the charge dynamics in the aged oil sample under such a highly enhanced electric field can also inject a large number of homocharges into the insulation system to neutralize the heterocharges remaining in the insulation system. This process may be very fast and be completed during the data acquisition process of the PEA system (about 30 s). Therefore, such rapid space charge dynamics are difficult to correctly record by using the current data acquisition system. However, on the basis of previous results obtaied under a pure DC electric field, the space charge distributions in the aged oil sample under 20 kV/mm with different polarity reversal durations can be estimated. As shown in Fig. 8(a), the estimated space charge profiles with different T_{pr} values show a similar trend to the results for 12 kV/mm, i.e., the amount of heterocharges and the peak of the ground electrode rapidly decrease when a longer polarity reversal duration T_{pr} is applied. As the charge decays exponentially with time, the peak of the ground electrode decreases from 15 to 9.3 C/m^3 when T_{pr} increases from 30 s to 2 min. It further decreases to 8.5 C/m^3 when T_{pr} increases to 5 min. The experimentally recorded space charge profile with a polarity reversal duration of 30 s is also shown in Fig. 8(a) for comparison. A small peak of heterocharges can be observed in the insulation system. Figure 8(b) shows the electric field distributions in the aged oil sample calculated from the space charge profiles in Fig. 8 (a). When T_{pr} is 30 s, a significant distortion of the electric field distributed in the oil gap and pressboard can be observed. The maximum electric field in the oil gap is about 42 kV/mm. When the polarity reversal duration increases to 2 min, the maximum electric field in the oil gap drops sharply to 27.2 kV/mm, and it further decreases to 26.6 kV/mm when T_{pr} is 5 min. The electric field enhancement in the oil gap under each condition is calculated and shown in Table 6.

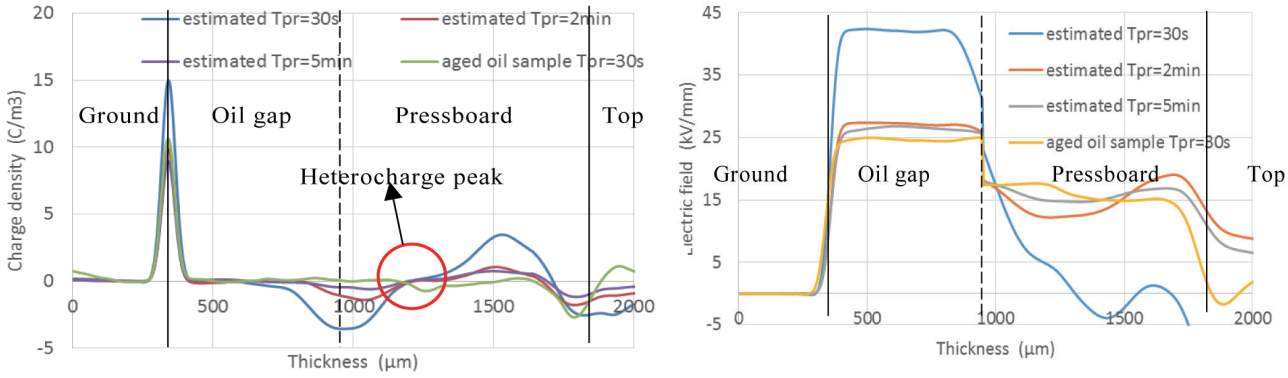

Fig. 8. (Color online) Estimated space charge (a) and electric field (b) distributions immediately after the first polarity reversal in the aged oil sample under 20 kV/mm with T_{pr} = 30 s, 2 min, and 5 min.

Table 6
Impacts of the duration of polarity reversal in the aged oil sample under 20 kV/mm.

Duration T_{pr} (min)	Peak of ground electrode (C/m^3)	Maximum electric field (kV/mm)	Field enhancement in oil gap (%)
0.5	15	42.1	110.5
2	9.3	27.2	36
5	8.5	26.6	33

Table 7
Impacts of the polarity reversal duration on the electric field enhancement.

Duration T_{pr} (min)	Electric field enhancement (%)		
	Fresh oil sample 20 kV/mm	Aged oil sample 12 kV/mm	Estimated aged oil sample 20 kV/mm
0.5	31.5	71.7	110.5
2	35.5	45.8	36
5	37	33.3	33

Table 7 shows the impacts of the polarity reversal duration on the electric field enhancement in the oil gap in both the fresh and aged oil samples under 12 and 20 kV/mm. The results clearly show that a longer polarity reversal duration has very limited impact in the fresh oil sample. In contrast, for the aged oil sample, the electric field enhancement can be effectively controlled by increasing the polarity reversal duration, i.e., 5 min is sufficient to reduce the electric field enhancement to less than 33% in the oil gap (only a displacement field exists).

However, space charge accumulation and dynamics also strongly depend on the voltage application time. The results of the long-duration measurement in the fresh oil sample (refer to Ref. 6) show that more than 24 h is required to reach the steady state in the fresh oil sample (the space charge accumulation reaches saturation). In this study, the voltage application duration is only 1 h, which means that the charge amount may be much less than that after the steady state. Therefore, the electric field enhancement in the long-duration fresh oil gap could potentially be much higher than the current results (< 40%) as more space charges accumulate in the insulation system and may result in unexpected risks.

5. Conclusions

In this paper, the space charge dynamics in an oil gap combined with a single-layer pressboard insulation system before and after a polarity reversal voltage is applied are investigated by the PEA method. The impacts of aged oil, the magnitude of the applied electric field and the polarity reversal duration are examined. A proposed space charge dynamics model before and after the polarity reversal operation has been experimentally proved, which allows us to estimate the space charge distribution immediately after polarity reversal based on the on-voltage and decay results under a DC electric field. Some important conclusions are summarized as follows:

1. For the fresh oil sample, the electric field enhancement in the oil gap is generally smaller than 10% immediately after the application of the reversed voltage, due to the very slow charge movement. A much higher field enhancement may occur in the long duration test.
2. For the aged oil sample, the electric field enhancement in the oil gap is much higher (more than 110%) immediately after polarity reversal. However, as the charge movement is greatly enhanced by the aged oil, a longer polarity reversal duration, T_{pr}, can greatly reduce the electric field enhancement.
3. The proposed estimation method has been validated. More accurate space charge distributions and electric field enhancements can be obtained by using the estimation method, particularly in the case of aged oil samples, as the charge neutralization is too rapid to be recorded.
4. The results of this study suggest that a longer voltage application time (> 24 h) is required for polarity reversal test for new convertor transformers to ensure the steady state of space charge dynamics.

Acknowledgments

The authors are grateful for the financial support from the State Grid Cooperation of China: Science and Technology Project of SGCC [SGRIZLJS (2014) 888].

References

1 U. Piovan: IEEE Int. Conf. Solid Dielectrics (ICSD) (2013).
2 W. Choo, G. Chen, and S. G. Swingler: 9th Int. Conf. Properties and Applications of Dielectric Materials (2009).
3 M. Abou-Dakka, A. Bulinski, and S. S. Bamji: IEEE Trans. Dielectr. Electr. Insul. **20** (2013) 654.
4 M. Fu, L. A. Dissado, G. Chen, and J. C. Fothergill: IEEE Trans. Dielectr. Electr. Insul. **15** (2008) 851.
5 M. Hao, Y. Zhou, G. Chen, G. Wilson, and P. Jarman: IEEE Trans. Dielectr. Electr. Insul. **22** (2015) 72.
6 M. Hao, Y. Zhou, G. Chen, G. Wilson, and P. Jarman: IEEE Trans. Dielectr. Electr. Insul. **23** (2016) 848.
7 M. Jeroense and P. Morshuis: IEEE Electr. Insul. Mag. **13** (1997) 26.
8 R. Ciobanu, I. Prisecaru, and C. Schreiner: IEEE Int. Conf. Solid Dielectrics (ICSD) (2004).
9 C. Tang, G. Chen, M. Fu, and R. Liao: IEEE Trans. Dielectr. Electr. Insul. **17** (2010) 778.
10 J. Hao, G. Chen, R. Liao, L. Yang, and C. Tang: IEEE Trans. Dielectr. Electr. Insul. **19** (2012) 1456.
11 Y. Zhou, Y. Wang, G. Li, N. Wang, Y. Liu, B. Li, P. Li, and H. Cheng: J. Electrostat. **67** (2009) 417.
12 K. Wu, Q. Zhu, H. Wang, X. Wang, and S. Li: IEEE Trans. Dielectr. Electr. Insul. **21** (2014) 1857.
13 R. Liu and C. Tomkvist: Electr. Insul. Dielectr. Phenom. Annu. Rep. (1995).
14 M. Huang, Y. Zhou, W. Chen, Y. Sha, and F. Jin: IEEE Trans. Dielectr. Electr. Insul. **21** (2014) 331.
15 B. Huang, M. Hao, J. Fu, Q. Wang, and G. Chen: IEEE Trans. Dielectr. Electr. Insul. **23** (2016) 881.
16 R. Bodega, P. H. F. Morshuis, and J. J. Smit: IEEE Trans. Dielectr. Electr. Insul. **13** (2006) 272.
17 IEC 61378-2:2001 Convertor transformers. Transformers for HVDC applications (2001).

About the Authors

Miao Hao was born in China in 1987. He received his B.Eng. degree (2009) from Xi'an Jiaotong University, China. He obtained his M.Sc. degree (2011) and Ph.D. degree (2015) from the University of Southampton. He is now a postdoctoral research fellow in the University of Southampton. His main research interests include space charge and ageing mechanisms in dielectrics for HVDC converter transformers and cables.

George Chen (SM'11) was born in China in 1961. He received his B.Eng. (1983) and M.Sc. (1986) degrees in electrical engineering from Xi'an Jiaotong University, China. After he obtained the Ph.D. degree (1990) from the University of Strathclyde, UK, on the permanent changes in the electrical properties of irradiated low-density polyethylene, he joined the University of Southampton as a postdoctoral research fellow and subsequently became a senior research fellow. In 1997, he was appointed as a research lecturer and promoted to a Reader in 2002. He is now a professor of high-voltage engineering at the University of Southampton and a visiting professor of Xi'an Jiaotong University. He has developed a wide range of interests in high-voltage engineering and electrical properties of materials and published over 300 papers. He is active in HVDC systems and involved with technical working groups in both IEEE and CIGRE.

Xin Chen received his M.S. degree in 1998 and Ph.D. degree in 2001 from Southeast University. He now is a professor and a research engineer of the Global Energy Interconnection Research Institute.

Chong Zhang received his M.S. degree in physical chemistry of high polymers in 2007 from Shanghai Jiaotong University. He now is a senior research engineer of the Global Energy Interconnection Research Institute SGCC. His reseach interests are in dielectric insulation materials of transform and transmission.

Wenpeng Li received his M.S. degree in materials science and engineering in 2010 from Xi'an Jiaotong University. He now is a senior research engineer of the Global Energy Interconnection Research Institute SGCC. His research interest is in dielectric insulation materials of the HVDC cable.

Haitian Wang (M'14) received his B.S. degree in computation mathematics and M.Eng. degree in electrical engineering from Sichuan University, Chengdu, China, in 1999 and 2003, respectively, and his Ph.D. degree in electrical engineering from Shanghai Jiaotong University, Shanghai, China in 2011. During 2011–2013, he held a postdoctoral position with China Electric Power Research Institute (CEPRI), Beijing, China. He was sponsored by the China Postdoctoral Science Foundation. In 2013, he joined the Global Energy Interconnection Research Institute SGCC. His research fields include electromagnetic analysis, VSC-HVDC transmission systems, and HVDC cables. He is the author or coauthor of more than 20 scientific papers and, so far, has seven papers that have been published in IEEE Transactions. He is a reviewer for IEEE Transactions on Power Delivery, Industry Applications, and IEEE Industry Applications Magazine.

Mingyu Zhou received his Diplom-Ingenieur degree in electrical engineering from the University of Karlsruhe (now KIT), Germany and is now a Ph.D. Candidate at Technische Universität Berlin (TUB), Germany. From 2009 to 2015 he worked with Südkabel (before 2004, ABB Energiekabel GmbH), Germany and was responsible for the development of cable accessories for 10–550 kV. Since October 2015, he has been the senior engineer for HVDC Cablesystem with the Global Energy Interconnection Reseach Institute Europe, Germany. His major research interest is on the development of and diagnostics for high-voltage cable systems (AC&DC).

Xianzhang Lei, Director General, GEIRI Europe GmbH of State Grid Corporation of China. He received his Ph.D. from Technische Universität Berlin in Germany and continued his post-doctorate at Yale University in the U.S.A. Afterwards he joined Siemens AG in Germany and served as Vice President of Asia Pacific in Power System. Since 2010, he has been working with State Grid Corporation of China. Professor Dr. Lei has published over 130 papers and possesses 14 patents in the fields of renewable energy and smart grids. He is a commissioner of the "AC/DC coordination control professional group", high-voltage DC and flexible AC transmission branch, CIGRE, and commissioner of the "power system planning and simulation professional group", high-voltage power system branch, CIGRE.